Three-Stage DRX Scheduling for Joint Downlink Transmission in C-RAN

Jia-Ming Liang, Ching-Kuo Hsu, Jen-Jee Chen, Kun-Ru Wu, and Yu-Chee Tseng

***Abstract*—Cloud-RAN (C-RAN) is a promising network architecture to provide 5G broadband services. In C-RAN, the base stations (BSs) are separated as the computation entities (i.e., *Baseband Units (BBUs)*) and the radio entities (i.e., *Remote Radio Heads (RRHs)*), where the BBUs are put in a centralized cloud to realize centrally control and the RRH are left at cell sites for signal transmission. With C-RAN, multiple collaborative cells can transmit data to *user equipments (UEs)* by *Joint Transmission (JT)* technology to improve network efficiency. On the other hand, 3GPP standard has defined the *Discontinuous Reception (DRX)* mechanism, which allows UEs to turn off their radio interfaces periodically to save their energy. However, how to cooperate DRX with JT under the C-RAN architecture is still an open issue. Therefore, this letter studies how to optimize UEs' DRX parameters while considering their *quality-of-service (QoS)* in C-RAN with JT. To solve this problem, we propose an energy-efficient JT scheduling scheme. The main idea of our scheme is to well pair UEs and BSs with the consideration of joint transmission quality and then optimizes DRX parameters to further save energy. Extensive simulation results show that our scheme can improve system throughput, well utilize resource and save UEs' energy consumption.**

***Index Terms*—5G mobile system, cloud radio access networks (C-RAN), joint transmission (JT), discontinuous reception (DRX), sleep scheduling.**

I. Introduction

CLOUD Radio Access Networks (C-RAN) is an emerging network architecture for 5G communications. With a centralized network architecture, the computation entities, i.e., *Baseband Units (BBUs)*, are separated from base stations (BSs), and put in a centralized cloud, and leaves *Remote Radio Heads (RRHs)* at cell sites. By this way, the radio resources of different RRHs can be centrally managed and multiple cells can be collaborated to improve network efficiency by the *Joint Transmission (JT)* technology [1]. On the other hand, *3GPP (the 3rd Generation Partnership Project)* has defined the *Discontinuous Reception (DRX)* mechanism, which allows UEs to turn off their radio interfaces when there is no data transmitted from *evolved Node B (eNB)*. However, how to optimize DRX parameters to minimize UEs' energy under the C-RAN architecture with JT is still an open issue. Thus, we address the DRX optimization problem under UEs' QoS constraints in C-RAN with JT. The objective is to schedule JT transmissions to improve network efficiency while minimizing UEs' wake-up periods to save energy under consideration of UEs' QoS requirements in terms of packet delay and data rate. To solve this problem, we propose an energy-efficient JT scheduling scheme. The key idea of our scheme is to pair the UEs with BSs by two special cost metrics and then optimize the corresponding DRX parameters to save energy.

In the literature [2], [3] propose dynamic point selection schemes to balance traffic load of RRHs; however, these works do not exploit JT to improve transmission efficiency. References [4], [5] consider C-RAN using JT. A cooperative caching placement for JT with single cell transmission to minimize UEs' data transmission time is proposed in [4]. The study [5] presents a beamforming design for Gaussian broadcast channels to maximize spectral efficiency. However, these works [4], [5] do not consider the optimization of throughput and energy simultaneously. Reference [6] presents a JT scheme with a *call admission control (CAC)* to maximize network throughput. The work [7] proposes a load-aware JT scheme to maximize coverage and ergodic link throughput. The study [8] develops a semi-dynamic cluster scheme to maximize energy efficiency. The work [9] proposes a power-factorizing mechanism to achieve the maximization of edge UEs' throughput. However, these works [6]–[9] do not consider the DRX mechanism, which can further save UEs' energy.

II. System Model

A. C-RAN and JT

Towards 5G, C-RAN is a promising architecture for mobile networks to support collaborative transmissions. C-RAN separates a traditional base station into two parts: digital function unit known as BBU and radio function unit known as RRH. BBUs are placed in the BBU pool in a cloud and connect with RRHs via optical fibers. It thus centralizes control. In C-RAN, JT is a way to realize collaborative transmissions and enhance data rate of UEs [1]. When a UE locates in the borders of multiple cells, JT can allocate multiple RRHs to serve it simultaneously. In Fig. 1(a), where $Cell_1$ and $Cell_2$ together serve UE_1, UE_2, and UE_3; without cooperative transmission by JT, UE_1 needs to receive data from $Cell_1$ at time slots 1∼2 and switches to $Cell_2$ at time slots 3∼4. Note that UE_2 and UE_3 are allocated at the same time slots because the transmissions are interference-free and the cells are centrally controlled by C-RAN. Thus, it requires 6 subframes to serve all UEs. In Fig. 1(b), with cooperative transmission by JT, UE_1 can receive data from $Cell_1$ and $Cell_2$ at time slots simultaneously.

Manuscript received July 29, 2019; accepted September 14, 2019. Date of publication September 24, 2019; date of current version February 7, 2020. This work was supported in part by the Ministry of Science and Technology under Grant 107-2221-E-024-001-MY3, Grant 105-2221-E-182-051, and Grant 106-2221-E-182-015-MY3, in part by the Ministry of Education Aiming for the Top University and Elite Research Center Development Plan (MOE ATU plan), in part by the Delta Electronics, in part by the Industrial Technology Research Institute (ITRI), in part by the Institute for Information Industry, in part by the Academia Sinica, and in part by the Chang Gung Memorial Hospital, Taoyuan. The associate editor coordinating the review of this article and approving it for publication was M. Dong. *(Corresponding author: Jen-Jee Chen.)*

J.-M. Liang is with the Department of Computer Science and Information Engineering, Chang Gung University, Taoyuan 33302, Taiwan, and also with the Department of General Medicine, Chang Gung Memorial Hospital, Taoyuan 33378, Taiwan (e-mail: jmliang@mail.cgu.edu.tw).

C.-K. Hsu, K.-R. Wu, and Y.-C. Tseng are with the Department of Computer Science, National Chiao Tung University, Hsinchu 30010, Taiwan (e-mail: hsuck@cs.nctu.edu.tw; kunruwu@cs.nctu.edu.tw; yctseng@cs.nctu.edu.tw).

J.-J. Chen is with the College of Artificial Intelligence, National Chiao Tung University, Hsinchu 30010, Taiwan (e-mail: jenjee@nctu.edu.tw).

Digital Object Identifier 10.1109/LWC.2019.2943471

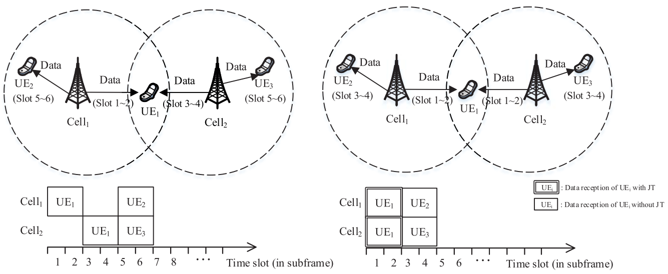

(a) Transmission without using JT. (b) C-RAN with JT.

Fig. 1. An example of joint transmission (JT) in C-RAN.

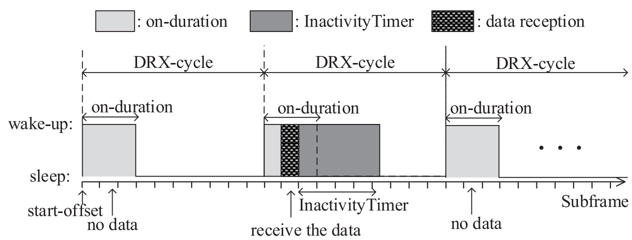

Fig. 2. An example of the DRX mechanism.

It only requires 4 subframes to serve all UEs, thus improving transmission efficiency.

B. DRX Mechanism

The DRX mechanism is designed to enhance downlink energy consumption of UEs. The DRX configurations, which are determined by eNB, are UE-specific. The UE performs wake-up/sleep operations in a periodic cycle when DRX is activated. An example is shown in Fig. 2. The basic duration is a subframe (with the length of 1 ms). There are short and long DRX cycles, and we focus on short DRX cycles only in the rest of this letter. Four parameters are defined when DRX is enabled: 1) *DRX-cycle-length*, 2) *DRX-start-offset*, 3) *on-duration*, and 4) *InactivityTimer*. The period of the UE to receive data from the eNB is called *DRX-cycle-length*. The starting subframe of DRX-cycle-length is called *DRX-start-offset*. The time when the UE has to stay awake to monitor any data delivered from the eNB is called *on-duration*. The UE starts *InactivityTimer* if any data is received, and stays awake before the timer expires. If any data is received, the timer is reset. When the timer expires, the UE turns off its radio interface and goes to sleep to reduce energy consumption. Before the next on-duration arrives, any data for the UE will be buffered at the eNB during the UE's sleep period. Note that the results of JT scheduling will strongly affect UEs' data reception behaviors as well as DRX configurations. Since JT scheduling can improve spectrum efficiency while DRX technique can save UEs' energy. We need to consider both of these factors to achieve better performance.

C. Problem Definition

We consider the downlink transmission under the TDD mode in C-RAN. There are N UEs with JT capability in M RRHs, where one or multiple serving cells may cover UE_i, $i = 1 \dots N$, denoted by set $Cell_i^{set}$, and each has a delay constraint of D_i (ms) and an admitted data rate of $R_i \geq 0$ (bits/ms). Channel quality determines the actual data bits that can be delivered; thus, we use C_i (bits/ms) as the channel rate between $Cell_i^{set}$ and UE_i. Our goal is to determine the downlink scheduling between N UEs and M cells and the adequate DRX parameters for each UE_i, including DRX-cycle-length (T_i), DRX-start-offset (Z_i), on-duration (O_i) and InactivityTimer (I_i), such that UEs can be served without violating their admitted data rate R_i and delay constraint D_i; meanwhile, the total number of wake-up subframes of UEs is minimal.

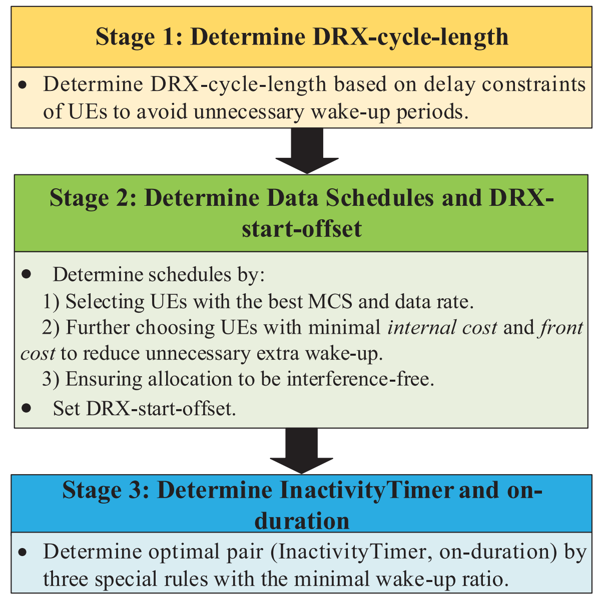

Fig. 3. Workflow of our proposed scheme.

III. Proposed Scheme

In this section, we present our energy-efficient JT scheduling algorithm to solve this problem. For each UE_i, we will determine its DRX parameters T_i, Z_i, O_i, and I_i. Our scheme maintains three key properties to improve system throughput and energy efficiency. First, we make all UEs' DRX-cycle-length be an integer multiple of others' to reduce unnecessary wake-up time of UEs caused by resource competition. Second, we carefully schedule UEs' transmission orders to reduce their unnecessary wake-up time. Finally, we optimize UEs' on-duration and InactivityTimer to minimize the expected wake-up ratios to further save energy. The workflow of the proposed scheme is shown in Fig. 3.

A. Stage 1: Determining DRX-Cycle-Length (T_i)

To decide each UE_i's T_i, the first step is to sort their delay constraints. Let $D_1 \leq D_2 \leq \cdots \leq D_N$ with no loss of generality. Then, let $T_1 = D_1 - 1$ and determine T_i, $i = 2 \dots N$, with the following formula:

$$T_i = \left\lfloor \frac{D_i}{T_{i-1}} \right\rfloor \times T_{i-1}. \qquad (1)$$

Eq. (1) makes $T_i < D_i$ for each UE_i, $i = 1 \dots N$, which guarantees the receiving data not to violate UEs' delay constraint. At the same time, Eq. (1) makes T_i be an integer multiple of T_{i-1}, for $i = 2 \dots N$, which can help UEs to interleave their wake-up periods to avoid resource competition. The allocation results will repeat after T_N / T_1 cycles.

Then, we classify the UEs according to DRX-cycle-length based on the above results and sort them based on their cycle-length in an ascending order. Thus, we have X classes of UEs with no loss of generality, denoted by $class_x$, $x = 1 \ldots X$, with DRX-cycle-length L_x. Stage 2 will schedule these classes of UEs sequentially.

B. Stage 2: Determining Data Schedules and DRX-Start-Offset (Z_i)

The main idea is to select the UEs with higher MCS and data rate first, and then apply two special cost metrics to better select serving cell-UE pairs in order to better utilize resource and serve more UEs. Let f^{cur} be the subframe index which is currently available to serve UEs; initially, $f^{cur} = 1$. Then, let $InfCell_{f^{cur}}$ be the cells that will cause interference to the current allocation results at subframe f^{cur}; initially, $InfCell_{f^{cur}} = \phi$. Denote by $subframe^{Alloc}_{i,j,k} \in \{0, 1\}$ the scheduling matrix: $Cell_j$ serves UE_i at subframe k if $subframe^{Alloc}_{i,j,k} = 1$; otherwise, $subframe^{Alloc}_{i,j,k} = 0$. Initially, $subframe^{Alloc}_{i,j,k} = 0$ for all *i*, *j*, and *k*. Then, we use UE^{UnServ} to be the set of UEs that have not been served; initially, $UE^{UnServ} = \{UE_i | UE_i \in class_x\}$, and UE^{UnServ}_j to be the set of UEs that have not been served by $Cell_j$; initially, $UE^{UnServ}_j = \{UE_i | UE_i \in class_x, Cell_j \in Cell^{set}_i\}$, for $j = 1 \ldots M$. Then, we use UE^{JT} to be the set of UEs that can exploit JT. Then, we let S^{Alloc}_i be the number of subframes that needs to allocate to UE_i and $S_{i,j} = \lceil \frac{R_i \times T_i}{\overline{C_i} - 3\sigma_i} \rceil$ be the estimated number of subframes for the serving cell $Cell_j \in Cell^{set}_i$ to serve UE_i, where $R_i \times T_i$ is the total data bits that will arrive during UE_i's cycle T_i, and $\overline{C_i} - 3\sigma_i$ is the worst channel rate which is acquired from historical information, where $\overline{C_i}$ and σ_i are the mean and deviation of UE_i's channel rate, respectively. Then, we let $s_{i,j} = 1$ be the service time unit in the scheduling. We also define $subframe^{Start}_{i,j,l}$ as the start subframe number of the *l*-th service time unit that $Cell_j$ allocates RBs to UE_i; initially, $subframe^{Start}_{i,j,l} = 0$ for all *i*, *j*, and *l*. In the following, we will determine the data scheduling of UEs and their DRX parameters in this stage. The details are depicted as follows.

Step 1: For the subframe f^{cur}, we find the UEs with the better MCS level as the candidate UEs, i.e.,

$$UE^{cand} = \{UE_i | UE_i = argmax_{i'}\{MCS_{i'} | UE_{i'} \in UE^{UnServ}\}\}. \quad (2)$$

Step 2: For the UEs in UE^{cand}, we select the UEs with the better data rate R_i, i.e.,

$$UE_{i*} = argmax_i\{R_i | UE_i \in UE^{cand}\}. \quad (3)$$

Step 3: We define a metric function, called *internal cost* $IC_{i,j}$, to evaluate the number of extra wake-up subframes that will be incurred when we schedule $s_{i,j}$, i.e.,

$$IC_{i,j} = |UE^{Sch}| \times s_{i,j}, \quad (4)$$

where $UE^{Sch} = \{UE_{i'} | i' \in (UE^{UnServ}_j - UE_i), S^{Alloc}_{i'} > 0\}$ is the set of UEs which have been scheduled partly of their serving time and $s_{i,j}$ is the service time unit in the scheduling. Then, we find the cell-UE pairs with the minimal $IC_{i,j}$ as follows:

$$(Cell_{j*}, UE_{i*}) = argmin_{i,j}\{IC_{i,j} | UE_i \ from \ \text{Eq. (3)}, \ Cell_j \in Cell^{set}_i, Cell_j \notin InfCell_{f^{cur}}\}. \quad (5)$$

Step 4: We define the second metric function, called *front cost* $FC_{i,j}$, to evaluate the extra subframes that will be incurred in front of the scheduling results of un-served UEs when scheduling $s_{i,j}$, i.e.,

$$FC_{i,j} = \sum_{j' \in Cell^{set}_i} |UE^{UnServ}_{j'} - UE_i| \times s_{i,j}. \quad (6)$$

Then, we find the cell-UE pairs with the minimal $FC_{i,j}$ as follows:

$$(Cell_{j*}, UE_{i*}) = argmin_{i,j}\{FC_{i,j} | (Cell_j, UE_i) \text{ from Eq. (5) }\}. \quad (7)$$

Step 5: Now, check if the chosen pair ($Cell_{j*}$, UE_{i*}) can be scheduled data without causing interference to other existing pairs in subframe f^{cur}. That is, if $subframe^{Alloc}_{i*,j,f^{cur}} = 0$ for all $Cell_j \in Cell^{set}_{i*}$, we allocate $s_{i*,j*}$ for the pair ($Cell_{j*}$, UE_{i*}) at subframe f^{cur} (where $Cell_{j*}$ includes all $Cell_j \in Cell^{set}_{i*}$ if $UE_{i*} \in UE^{JT}$), update the scheduling matrix by $subframe^{Alloc}_{i*,j*,f^{cur}+y \cdot L_x} = 1$, and update the interfering cell set by $InfCell_{f^{cur}+y \cdot L_x} = InfCell_{f^{cur}+y \cdot L_x} \cup Cell^{set}_{i*}$, for $y = 0 \ldots (\frac{L_X}{L_x} - 1)$. Then, mark the start point of pair $(Cell_{j*}, UE_{i*})$ by $subframe^{Start}_{i*,j*,l} = f^{cur}$ if $Cell_{j*}$ serves UE_{i*} for the *l*-th service time unit at subframe f^{cur}, update the total allocated subframes by $S^{Alloc}_{i*} = S^{Alloc}_{i*} + 1$, and set $S_{i*,j*} = S_{i*,j*} - 1$. Then, remove UE_{i*} from UE^{UnServ} and UE^{UnServ}_{j*} if $S_{i*,j*} = 0$. Otherwise, if causing interference, add $Cell_{j*}$ to $InfCell_{f^{cur}}$ and go back to step 1 to find the next candidate pair.

Step 6: Based on above results, we set the DRX-start-offset Z_i for each UE_i, $i = 1 \ldots N$, by

$$Z_i = min\{subframe^{Start}_{i,j,1} | Cell_j \in Cell^{set}_i\}. \quad (8)$$

To summarize, Stage 2 determines the allocation of serving cell-UE pairs and the DRX-start-offset Z_i for each UE_i, $i = 1 \ldots N$.

C. Stage 3: Optimizing DRX Parameters (I_i and O_i)

The goal of this stage is to determine the best InactivityTimer I_i and on-duration O_i for each UE_i, $i = 1 \ldots N$, to reduce the unnecessary wake-up periods. Recall that $subframe^{Start}_{i,j,l}$ is the start subframes determined in Stage 2. Below, we calculate wake-up ratio for each UE_i's I_i and O_i based on [10]. Specifically, we first define ER^{WakeUp}_i to represent the expected wake-up ratio of UE_i with its I_i and O_i. Then, we design three rules for determining their values. Finally, we choose the best pair which incurs the minimal expected wake-up ratio for each UE_i. The details are as follows.

First, we define ER^{WakeUp}_i by calculating the expected number of wake-up subframes over the DRX-cycle-length T_i for UE_i, i.e., $ER^{WakeUp}_i = \frac{max\{(max_{j,l}\{EPO_{i,j,l} | Cell_j \in Cell^{set}_i\} - Z_i), O_i\} + I_i}{T_i}$, where $EPO_{i,j,l} = (subframe^{Start}_{i,j,l} + 1)$ is the *l*-th expected end subframe for the pair ($Cell_j$, UE_i).

Second, we design three rules to find feasible (I_i, O_i). Then, we choose the best pair which has the minimal expected wake-up subframes.

- *Rule 1:* Set $I_i = 0$ and $O_i = max_{j,l}\{subframe^{Start}_{i,j,l} + s_{i,j} | Cell_j \in Cell^{set}_i\} - Z_i$.

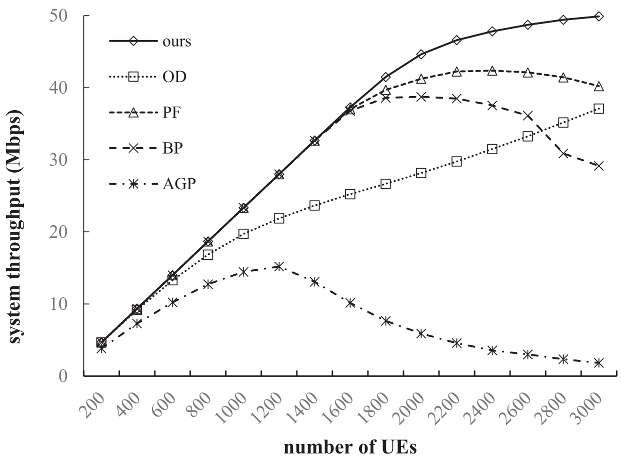

Fig. 4. Comparisons on system throughput.

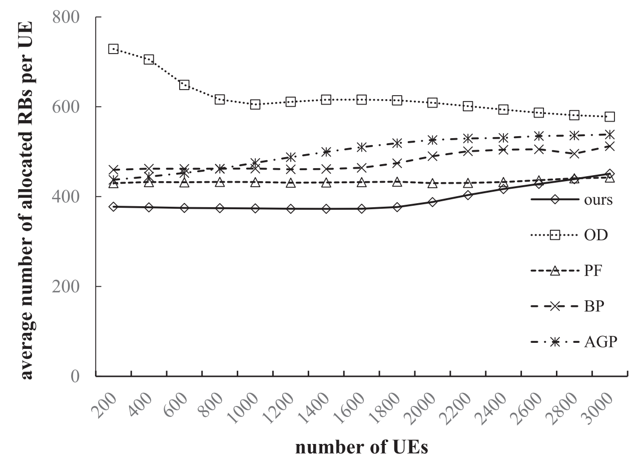

Fig. 5. Comparisons on average number of allocated RBs per UE.

- *Rule 2:* Set $I_i = 1$ and $O_i = (max_{j,l>1} \{subframe_{i,j,l}^{Start} | Cell_j \in Cell_i^{set}, subframe_{i,j,l}^{Start} - subframe_{i,j,l-1}^{Start} > 1\} - Z_i) + 1$.
- *Rule 3:* Set $I_i = max\{h_{i,k}\} + 1$ and $O_i = min_{j,l}\{subframe_{i,j,l}^{Start} + s_{i,j} | Cell_j \in Cell_i^{set}\} - Z_i$, where $h_{i,k}$ is the k-th idle period of UE_i.

Note that Rule 1 favors shorter InactivityTimer and longer on-duration, Rule 2 favors longer InactivityTimer and shorter on-duration, and Rule 3 ensures UEs to get all data from separated wake-up periods. Based on these rules, we can evaluate the expected wake-up ratio and choose the best pair with the minimal expected wake-up ratio.

IV. Simulation Results

In this section, we develop a simulator in C++ to verify the effectiveness of our scheme. The simulation parameters are following [11]. Three types of traffic are adopted in the simulation, including HTTP (256 Kbps, 300 ms), VoIP (512 Kbps, 150 ms), and video streaming (1 Mbps, 100 ms) [12], [13]. The numbers of cells and UEs are $M = 25$ and $N = 200{\sim}3000$, respectively. Note that the UEs are distributed uniformly and move randomly with the speed of 1.4 m/s [14].

In the simulation, we compare our scheme against ***offloading-aware dynamic point selection scheme (OD)*** [3], ***altruistic-game based scheme (AGP)*** [4], ***blocking-probability aware scheme (BP)*** [6], and ***power-factorizing based scheme (PF)*** [9]. **OD** offloads data of UEs from hotspot to neighbouring cells to improve spectrum utilization. **AGP** minimizes data transmission time of UEs based on a strategy of local altruistic game. **BP** exploits a call blocking probability to improve system performance. **PF** schedules cell-edge UEs in advance to well leverage joint transmission. Since **PF** and **BP** neglect to design subframe-level scheduling, we apply ***round-robin*** scheduling (same as **AGP**) to them. Note that each simulation result is averaged by at least 2000 experiments.

A. System Throughput

First, we investigate the effects of the number of requested UEs on system throughput. As shown in Fig. 4, **AGP** has lower throughput because it neglects to consider achievable transmission quality and data rate of UEs. **BP** is higher than **OD** and **AGP** because it leverages a call blocking probability to improve performance. **PF** is better than above them because it serves cell-edge UEs first to potentially leverage joint transmission. Our scheme outperforms them because it well considers the joint transmission quality to improve transmission rate and exploits two special cost metrics to better determine the scheduling orders and utilize resource.

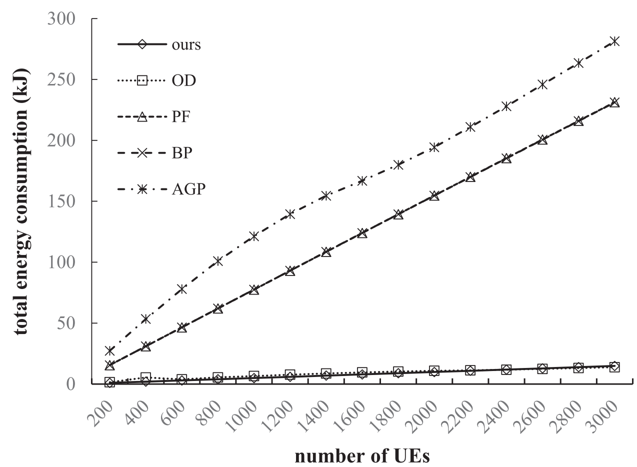

Fig. 6. Comparisons on total energy consumption.

B. Average Allocated RBs Per UE

Second, we investigate the effects of the number of UEs on average number of allocated RBs per UE. As shown in Fig. 5, **OD** needs the most RBs because it neglects to exploit JT to improve achievable transmission rate. **PF** needs less resource than **BP** and **AGP** because the cell-edge UEs are served first and thus can better elaborate joint transmission. Our scheme outperforms them because it well pairs the cells and UEs to improve the joint transmission efficiency and schedule data concentratedly and periodically to potentially reduce the allocated resource.

C. Total Energy Consumption

Next, we investigate the effects of the number of UEs on total energy consumption. The energy model is referred to [15], where the consumed energy for active status with data receiving (wake-up), without data receiving (idle) and sleep period are 500 mW, 255.5 mW, and 11 mW per subframe, respectively. As shown in Fig. 6, the total energy consumption increases as the number of UEs increases. Our scheme has the lowest energy consumption because it finds the best pairs

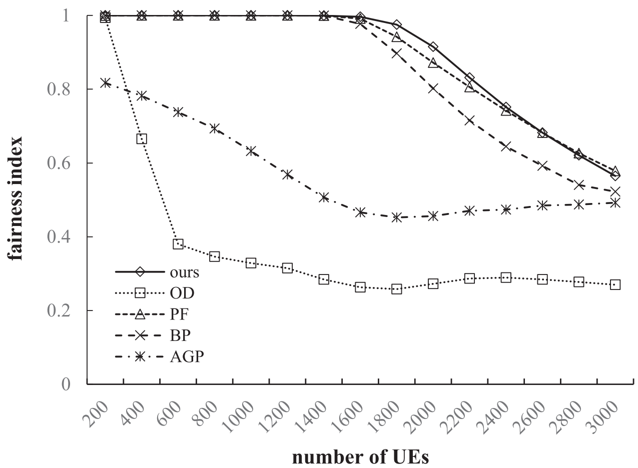

Fig. 7. Comparisons on fairness index.

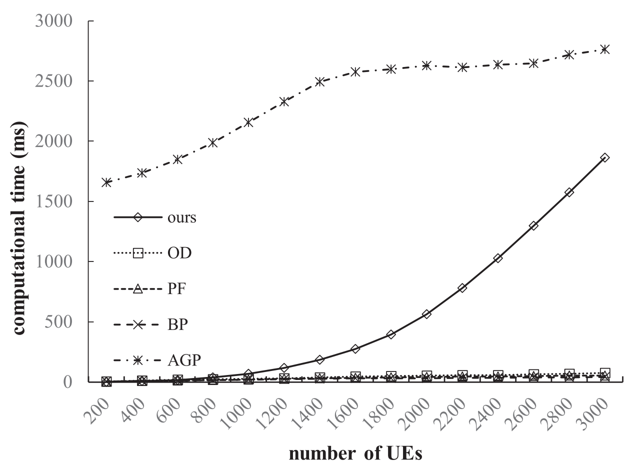

Fig. 8. Comparisons on computational time.

of cells and UEs to improve transmission rate which potentially reduces the wake-up time of UEs for data reception. In addition, it also leverages two special cost metrics to facilitate DRX optimization to further save energy. Contrarily, most of the other schemes neglect to optimize DRX parameters when scheduling. Although **OD** has similar energy consumption to our scheme, our scheme exploits joint transmission that can further improve throughput.

D. Fairness

Here, we investigate the effects of the number of UEs on fairness under a highly congested network, where there are 200$\sim$3000 UEs. Note that the network becomes saturated as the number of UEs increases; thus, it is impossible to get a fairness index of 1, because the network resource is not enough to satisfy the requirements of all UEs. As shown in Fig. 7, **OD** and **AGP** incur the lowest index because they neglect to consider joint transmission efficiency and the satisfaction rate of UEs. **PF** has higher index than **BP** because it serves cell-edge UEs first to potentially avoid starvation. Our scheme has the highest index because it finds the best pairs of cells and UEs and better determines the schedule orders which can avoid starvation.

E. Computational Complexity

We then investigate the effects of the number of UEs on the computational time. The time is measured by the platform of Dell 990 with Intel i7-2600 3.4GHz and DDR3-1600 16GB. As shown in Fig. 8, the computational time of most schemes increases when the number of devices increases. Comparing with our scheme, **OD**, **PF**, and **BP** have lower computational time because they neglect to consider UEs' QoS and network efficiency. Our scheme has higher computational time because it needs more time to find the best pairs of cells and UEs with better spatial reuse efficiency to ensure UEs' QoS and improve network efficiency.

V. Conclusion

We have addressed the DRX optimization problem by considering UEs' QoS requirements in C-RAN with JT. We proposed an energy-efficient JT scheduling which has three stages. The DRX cycle is determined in the first stage to reduce unnecessary wake-up periods and avoid resource competition. The data allocation order is determined in the second stage, which is based on UEs' MCS levels and achievable data rate. Three special rules are adopted in the third stage, with which the DRX parameters can be further optimized. Extensive simulation results show that our scheme can improve system throughput, well utilize resource and save UEs' energy consumption. In the future work, we will continue to study a new methodology based on artificial intelligence to further optimize JT scheduling with DRX.

References

[1] R. Irmer *et al.*, "Coordinated multipoint: Concepts, performance, and field trial results," *IEEE Commun. Mag.*, vol. 49, no. 2, pp. 102–111, Feb. 2011.

[2] C.-K. Hsu, J.-M. Liang, K.-R. Wu, J.-J. Chen, and Y.-C. Tseng, "Energy-efficient dynamic point selection for cloud radio access networks (C-RAN)," in *Proc. IEEE WCNC*, Mar. 2017, pp. 1–6.

[3] C.-K. Hsu, J.-M. Liang, J.-J. Chen, K.-R. Wu, and Y.-C. Tseng, "Data offloading for dynamic point selection in cloud radio access networks (C-RAN)," in *Proc. IEEE WCNC*, Apr. 2018, pp. 1–6.

[4] H. Li, C. Yang, X. Huang, N. Ansari, and Z. Wang, "Cooperative RAN caching based on local altruistic game for single and joint transmissions," *IEEE Commun. Lett.*, vol. 21, no. 4, pp. 853–856, Apr. 2017.

[5] K. Kwak, H. W. Je, S.-H. Park, and S. Choi, "CoMP joint transmission for Gaussian broadcast channels in delay-limited networks," *IEEE Trans. Veh. Technol.*, vol. 66, no. 3, pp. 2053–2058, Mar. 2017.

[6] S.-Y. Kim and C.-H. Cho, "Call blocking probability and effective throughput for call admission control of CoMP joint transmission," *IEEE Trans. Veh. Technol.*, vol. 66, no. 1, pp. 622–634, Jan. 2017.

[7] C.-H. Liu and P.-C. Chen, "Load-aware coordinated multipoint joint transmission in dense heterogeneous networks: Downlink coverage and throughput limits," in *Proc. IEEE ICC*, May 2017, pp. 1–7.

[8] Y. Li, W. Jia, B. Cao, C. Wang, and M. Daneshmand, "Energy-efficient cluster division for multi-cell joint transmission technology," *Wireless Commun. Mobile Comput.*, vol. 16, no. 17, pp. 3045–3055, Oct. 2016.

[9] S. Fu, H. Wen, and B. Wu, "Power-fractionizing mechanism: Achieving joint user scheduling and power allocation via geometric programming," *IEEE Trans. Veh. Technol.*, vol. 67, no. 3, pp. 2025–2034, Mar. 2018.

[10] J.-M. Liang, J.-J. Chen, P.-C. Hsieh, Y.-C. Tseng, "Two-phase multicast DRX scheduling for 3GPP LTE-advanced networks," *IEEE Trans. Mobile Comput.*, vol. 15, no. 7, pp. 1839–1849, Jul. 2016.

[11] P.-M. Hsu, J.-J. Chen, and J.-M. Liang, "Dynamic cooperating set planning for coordinated multi-point (CoMP) in LTE/LTE-advanced systems," in *Proc. APNOMS*, Sep. 2013, pp. 1–6.

[12] J.-M. Liang, J.-J. Chen, H.-H. Cheng, and Y.-C. Tseng, "An energy-efficient sleep scheduling with QoS consideration in 3GPP LTE-advanced networks for Internet of Things," *IEEE J. Emerg. Sel. Topics Circuits Syst.*, vol. 3, no. 1, pp. 13–22, Mar. 2013.

[13] S. Gadgil, S. Ranjan, D. Joshi, M. Mehta, N. Akhtar, and A. Karandikar, "Performance evaluation and viability of IFOM in heterogeneous LTE–WLAN network," in *Proc. IEEE WCNC*, May 2015, pp. 1524–1529.

[14] T. Deng, X. Wang, P. Fan, and K. Li, "Modeling and performance analysis of a tracking-area-list-based location management scheme in LTE networks," *IEEE Trans. Veh. Technol.*, vol. 65, no. 8, pp. 6417–6431, Aug. 2016.

[15] S. Hailu, P. Lunden, E. Virtej, N. Kolehmainen, O. Tirkkonen, and C. Wijting, "DRX-aware power and delay optimized scheduler for bursty traffic transmission," in *Proc. IEEE Veh. Technol. Conf. (VTC)*, May 2015, pp. 1–5.